Monthly Notices of the ROYAL ASTRONOMICAL SOCIETY

MNRAS **503,** 4242–4249 (2021) doi:10.1093/mnras/stab545
Advance Access publication 2021 March 1

Is the Bremer Deep Field reionized, at $z \sim 7$?

J. M. Rodríguez Espinosa [1,2]★ J. M. Mas-Hesse[3] and R. Calvi[1,2]

[1]*Instituto de Astrofísica de Canarias, E-38205 La Laguna, Spain*
[2]*Departamento de Astrofísica, Universidad de La Laguna, E-38206 La Laguna, Spain*
[3]*Departamento de Astrofísica, Centro de Astrobiología (CSIC-INTA), E-28850 Madrid, Spain*

Accepted 2021 February 19. Received 2021 February 19; in original form 2020 December 3

ABSTRACT

We show herein that the population of star-forming galaxies in the Bremer Deep Field (BDF) has enough ionizing power to form two large ionized bubbles that could be in the process of merging into a large one with a volume of 14 000 cMpc^3. The sources identified in the BDF have been completed with a set of expected low-luminosity sources at $z \sim 7$. We have estimated the number of ionizing photons per second produced by the different star-forming galaxies in the BDF. This number has been compared with the number that would be required to ionize the bubbles around the two overdense regions. We have used, as reference, ionizing emissivities derived from the AMIGA (Analytic Model of Intergalactic-medium and Galaxies) cosmological evolutionary model. We find that even using the most conservative estimates, with a Lyman continuum escape fraction of 10 per cent, the two regions we have defined within the BDF would be reionized. Assuming more realistic estimates of the ionizing photon production efficiency, both bubbles would be in the process of merging into a large reionized bubble, such as those that through percolation completed the reionization of the Universe by $z = 6$. The rather small values of the escape fraction required to reionize the BDF are compatible with the low fraction of faint Ly α emitters identified in the BDF. Finally, we confirm that the low-luminosity sources represent indeed the main contributors to the BDF ionizing photon production.

Key words: galaxies: high-redshift – galaxies: starburst – early Universe.

1 INTRODUCTION

Many high-redshift sources are known from various surveys made in the past decades. Most of the detections have been done not only through broad-band searches (Steidel et al. 2005; Bouwens et al. 2010, 2006; Stark et al. 2010) but also with narrow-band filters tuned to the Ly α line (Ouchi et al. 2008, 2010; Chanchaiworawit et al. 2017). However, the number of spectroscopic confirmations of the sources detected in the various surveys is rather scarce (Castellano et al. 2018; Harikane et al. 2018; Calvi et al. 2019). In particular, Vanzella et al. (2011) discovered spectroscopically two sources in the Bremer Deep Field (BDF) at a redshift of 7. Furthermore, Castellano et al. (2018) detected an additional source at a similar redshift within the same field.

There are quite a few high-z protoclusters discovered in the past few years (Toshikawa et al. 2012; Castellano et al. 2016; Abdullah, Wilson & Klypin 2018; Harikane et al. 2018, 2019; Jiang et al. 2018; Oteo et al. 2018; Chanchaiworawit et al. 2019; Higuchi et al. 2019). Their importance in the reionization process has indeed been recognized. Interestingly, the relative fraction of volume occupied by protoclusters increases with z (Chiang et al. 2017). Besides, protoclusters represent a collection of sources that together could produce sufficient ionizing photons, such that a fraction of them could escape contributing to the reionization of the universe through the creation of ionized bubbles.

Papers discussing the presence of ionized bubbles are appearing more often lately; For example, Tilvi et al. (2020) show evidence of a bubble ionized by three Ly α emitting galaxies at $z = 7.7$. Also, Meyer et al. (2020) have found a double-peaked Ly α source producing its own ionized bubble at $z = 6.8$. We have also recently characterized an ionized bubble powered by a protocluster at $z \sim 6.5$ (Rodríguez Espinosa et al. 2020). Finally, Castellano et al. (2018) have explored the conditions around the three Ly α emitters (LAEs) they had identified in the BDF. While the detection of three LAEs at $z \sim 7$ would point to the presence of a large enough reionized bubble allowing for Ly α to escape, the non-detection of any Ly α emission from other 14 Lyman break galaxies (LBGs) identified in the field was apparently at odds with this scenario. Castellano et al. (2018) analysed the possibility that the three LAEs in the BDF could produce large ionized bubbles around them, concluding that only after a very long period of continuous star formation, and assuming rather large values of the ionizing continuum escape fraction, the ionized bubbles would reach such a size that Ly α photons would be able to escape the region unaffected by scattering in the intergalactic medium (IGM). They considered different options to explain the leakage of Ly α photons from only the three bright emitters, assuming that the faint LBGs could be more evolved or located in the outskirts of the overdense region, still surrounded by neutral gas.

In this paper, we re-examine the data in Castellano et al. (2018) to check whether the complete collection of sources in the two overdense regions of the BDF would be capable of reionizing two large bubbles around them. To this end, we have added the ionizing flux from all the sources in each of the two regions of the BDF,

★ E-mail: jmr.espinosa@iac.es

© 2021 The Author(s)
Published by Oxford University Press on behalf of Royal Astronomical Society

Downloaded from https://academic.oup.com/mnras/article/503/3/4242/6155040 by guest on 12 February 2026

including a set of still undetected, yet expected, low-luminosity sources.

As we will discuss later, cosmological evolutionary models require only very low values of the ionizing continuum escape fraction to explain the complete reionization of the universe by $z \sim 6$ (around 5–10 per cent on average). These low values of $f_{\rm esc,LyC}$ are compatible with low values of the Ly α photon escape fraction in the line of sight, as shown by Chisholm et al. (2018). As a good example, there is the prototypical LBG analogue Haro 11, with $f_{\rm esc,LyC} = 0.03$ and $f_{\rm esc,Ly\,\alpha} = 0.04$ reported by Verhamme et al. (2017). Chisholm et al. (2018) indeed considered that in scenarios with low extinction, both $f_{\rm esc,Ly\,\alpha}$ and $f_{\rm esc,LyC}$ should be intrinsically very similar, though the scattering of Ly α photons by neutral clouds yields a non-predictable behaviour of the Ly α emission (see e.g. Dijkstra, Gronke & Venkatesan 2016). If the $f_{\rm esc,Ly\,\alpha}$ values remain low, in line with the expected $f_{\rm esc,LyC}$ range, EW(Ly α) values would be well below the detection limit reported by Castellano et al. (2018) (around 30 Å at $z \sim 7$). Furthermore, while the destruction, by resonant scattering, of Ly α photons is a complex process, which depends largely on both the geometry and kinematics of the neutral gas close to the star-forming regions, we think that the lack of Ly α emission from the LBGs does not prevent the leakage of ionizing photons when the full solid angle is considered. Therefore, the LBGs could contribute, in a significant way, to the reionization of the IGM even if they do not show Ly α emission along the line of sight.

To estimate the size of the ionized bubbles in the BDF, we have considered the two pointings reported by Castellano et al. (2018). Then, we have derived the Ly α escape fraction of the three LAEs using the calibration by Sobral & Matthee (2019). Knowing the $f_{\rm esc,Ly\,\alpha}$ values and the Ly α fluxes from these three bright galaxies, we have derived the number of intrinsic ionizing continuum photons. As for the medium- and low-luminosity sources, their ionizing fluxes have been derived from the ultraviolet (UV) continuum using our own evolutionary models. Finally, we have used the AMIGA (Analytic Model of Intergalactic-medium and Galaxies) model (Salvador-Solé et al. 2017) to derive values of the expected ionizing emissivity at $z \sim 7$, with which we have compared the ionizing fluxes from the BDF.

Section 2 reviews the BDF field and the different sources within it. In particular, we have done an estimation of the number of low-luminosity sources, based on the surface density derived by Bouwens et al. (2015) at $z \sim 7$. Section 3 shows the derivation of the number of ionizing continuum photons produced by the different sources in the region. Finally, in Section 4 we use the expected emissivity at $z = 7$ from the AMIGA model (Salvador-Solé et al. 2017), and considering the volumes of both regions, we compute the minimum number of continuum ionizing photons required to ionize each region and explore the possible formation of an even larger reionized bubble enclosing most of the BDF. We finish with the conclusions in Section 5. All units are in concordance cosmology units, namely $\Omega_\Lambda = 0.7$, $\Omega_{\rm M} = 0.3$, and $H_0 = 70$ km s^{-1} Mpc^{-1}. Magnitudes are given in the AB system (Oke & Gunn 1983). For cosmological calculations, we have used the *CosmoCal* webtool kindly made available by Wright (2006), and the *Cosmological Calculator for a Flat Universe* built by Nick Gnedin at Fermilab (`https://home.fnal.gov/~gnedin/cc/`).

2 CHARACTERIZING THE OBSERVED BDF

The fields observed by Vanzella et al. (2011) and Castellano et al. (2018) were relatively small, around 0.7 × 0.7 pMpc^2 each, much smaller than the full BDF, which extends over 2.4 × 2.4 pMpc^2.

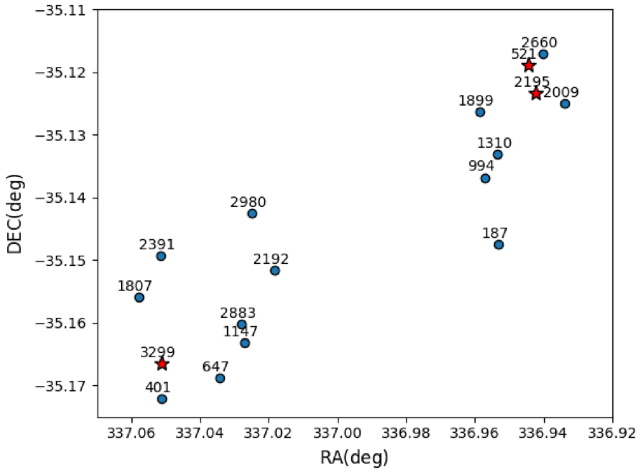


Figure 1. The two pointings can be noticed in this figure of the BDF galaxy distribution. The pointings were guided by the two LAEs discovered originally (Vanzella et al. 2011). The upper right one we will call Group 1, while Group 2 would be the bottom left one. The three LAEs are marked with solid red stars. The medium-luminosity LBGs are marked with blue circles.

The observations consisted of two pointings around BDF 521 and BDF 3299, respectively. In what follows, we will analyse separately the population of sources in these two pointings. As indicated in Castellano et al. (2016), each specific pointing covered 3.94 and 3.82 squared arcmin, respectively. Castellano et al. (2018) indicated that most of the galaxies identified should be within the redshift range (z) of 6.95–7.15. We have derived the volumes assuming the difference in distances between these limiting redshifts. Making use of the Cosmocalc (Wright 2006) and of the *Cosmological Calculator for a Flat Universe* by N. Gnedin, we arrive to the volumes of each of the two pointings, namely 1718 cMpc^3 for the region containing BDF 521 and 1660 cMpc^3 for the region containing BDF 3229 (see Fig. 1).

Within these two specific pointings, Castellano et al. (2018) found 17 sources, 3 of which are LAEs, while the rest are LBGs with no Ly α emission detected. For the three LAEs, there is spectroscopy (Vanzella et al. 2011; Castellano et al. 2018), from which we have used both the Ly α fluxes and their equivalent widths (EWs).

2.1 Number of low-luminosity sources in the BDF

Low-luminosity galaxies are recognized as key elements in the process of reionizing the Universe (Bouwens et al. 2015; Robertson et al. 2015; Rodríguez Espinosa et al. 2020). To derive the number of low-luminosity sources expected in the BDF, we have used the typical surface density values of high-redshift star-forming galaxies given in Bouwens et al. (2015) for the universe at $z \sim 7$, as listed in their appendix table A1. The surface density and number of sources are included, for completeness, in Table 1. Castellano et al. (2016) also claim that the overdensity in the observed field ranges from 3 to 4. Thus, we will assume an overdensity of 3.5 in what follows. Therefore, the derivation of the number of low-luminosity sources has been done multiplying the surface density, in number of sources per arcmin^2, by the surface of the observed fields, 3.94 and 3.82 arcmin^2, respectively. Then, the average number of low-luminosity sources in the BDF has been multiplied by 3.5, which is the average overdensity in the two small BD fields that we have assumed according to Castellano et al. (2016). The results are given in Table 1. Note that the lowest luminosity in this case, $m_{\rm AB} = 29.70$,

Downloaded from https://academic.oup.com/mnras/article/503/3/4242/6155040 by guest on 12 February 2026

Table 1. The number of expected low-luminosity sources in Group 1 and Group 2 of the BDF at $z \sim 7$. Columns: (1) magnitude range, (2) surface density from Bouwens et al. (2015, table A1), (3) the number of sources in Group 1, (4) the number of sources in Group 2, (5) the number of sources in Group 1 multiplied by the overdensity factor, which we take as 3.5, and (6) the number of sources in Group 2 corrected as well by the same overdensity factor (Castellano et al. 2016).

M_{AB} range	Surface density (arcmin^{-2})	# Group 1 (3.94 arcmin^2)	# Group 2 (3.82 arcmin^2)	# Corrected 1 overdensity	# Corrected 2 overdensity
27.45–27.95	0.831 ± 0.242	3.27 ± 0.92	3.17 ± 0.95	11.46 ± 0.85	11.11 ± 0.85
27.95–28.45	1.273 ± 0.300	5.02 ± 1.18	4.86 ± 1.15	17.55 ± 4.38	17.02 ± 4.14
28.45–28.95	1.264 ± 0.518	4.98 ± 2.04	4.83 ± 1.98	17.43 ± 7.14	16.90 ± 7.96
28.95–29.45	4.286 ± 0.953	16.37 ± 3.64	16.89 ± 3.75	57.10 ± 13.14	57.30 ± 13.91
29.45–29.95	3.484 ± 0.859	13.73 ± 3.38	13.31 ± 3.28	48.04 ± 11.85	46.58 ± 12.53

corresponds to an absolute rest-frame UV magnitude of $M_{UV} = -19.49$. It has been shown that there are no cut-offs in the UV luminosity function down to $M_{UV} \sim -15$ (Bouwens et al. 2017; Yue et al. 2018). Thus, the results obtained herein for the low-luminosity sources are rather conservative. Finally, we would like to mention that using the surface densities from Bouwens et al. (2015) we should expect to find barely one source brighter than 25.95. Note that, as expected, in the reduced BDF there is indeed only one source with $m_{AB} = 25.97$, which is BDF2883.

3 NUMBER OF IONIZING CONTINUUM PHOTONS FROM THE SOURCES IN THE BDF

To check whether the entire collection of sources reported in Castellano et al. (2018), with the addition of the low-luminosity sources that we have derived, is capable of producing two ionized bubbles or even a large one encompassing the whole region, we have first computed the number of ionizing continuum photons (1) from the three LAEs, (2) from the rest of the galaxies reported by Castellano et al. (2018), which we will call mid-luminosity sources, and (3) from the expected low-luminosity sources that we have derived from the field surface density at $z \sim 7$ (Bouwens et al. 2015).

3.1 Number of Lyman continuum (LyC) photons from the three LAEs in the BDF

There are three Lyα emitting galaxies in the BDF, two BDF521 and BDF3299, reported by Vanzella et al. (2011), and an additional one, BDF 2195, identified by Castellano et al. (2018). These three sources have redshifts derived from the spectroscopy, namely $z = 7.008$ for BDF521 and BDF2195 and $z = 7.109$ for BDF3299 (Vanzella et al. 2011; Castellano et al. 2018). Moreover, for these sources we have also the measured rest-frame EWs (EW$_o$; Castellano et al. 2018). To derive the number of ionizing photons emitted per second from the observed Lyα fluxes, we need first to estimate the Lyα escape fraction, $f_{esc,Ly\alpha}$. Sobral & Matthee (2019) derived a correlation between the Lyα EW and the escape fraction of high-redshift galaxies, yielding an empirical relation of both parameters. Using that relation, we have derived the values of $f_{esc,Ly\alpha}$ for the three LAEs. From the escape fractions and the observed Lyα fluxes, we get the intrinsic Lyα luminosities. Finally, we have computed the effective number of ionizing photons per second (Q^e_{ion}), i.e. the value corresponding to the intrinsic Lyα luminosities assuming case B conditions, using the expression $L(Ly\alpha) = 1.18 \times 10^{-11} \times Q^e_{ion}$ erg s^{-1} (Osterbrock 1989). This relation does not depend on the properties of the ionizing stars, nor on evolutionary models, but just on the physical conditions of the gas, and is based on a ratio $L(Ly\alpha)/L(H\alpha) = 8.7$ that is usually assumed for star-forming regions (see Dopita & Sutherland 2003; and Hayes 2019). The results are listed in Table 2. Note that the intrinsic number of LyC photons (Q^*_{ion}) being emitted by the massive stars will be larger by a factor of $1/(1 - f_{esc,LyC})$, since the escaping LyC photons do not participate in the ionization of the gas traced by the Lyα emission.

We want to remark that the correlation by Sobral & Matthee (2019) implies that the intrinsic values of the Lyα EWs converge in average around EW(Lyα) $\sim$ 200 Å. Indeed, most of the galaxies used to derive this correlation show intrinsic (once corrected from the escape fraction) EW(Lyα) values within the range of 150–250 Å. These high EW values can only be achieved when stars with very high ionizing power dominate the overall emission. We show in Fig. 2 (top) the predicted evolution of EW(Lyα) by Otí-Floranes & Mas-Hesse (2010) for a very short lived starburst and for a long-lasting episode forming massive stars at a constant rate during hundreds of Myr [a similar behaviour was presented by Charlot & Fall (1993) with a different set of models]. Values of EW(Lyα) above 200 Å are predicted only during the first ~3–4 Myr after the onset of a massive star formation episode, but they are not compatible with a starburst having formed stars at a stable rate during more than around 50 Myr, at least for metallicities above $Z \sim 0.008$. Most of the LAEs at high redshift analysed by Sobral & Matthee (2019) should therefore be experiencing very young massive star formation episodes or a sudden, recent increase of their otherwise lower, long-lasting star formation rate.

The ionizing power of a massive star cluster is generally defined in the literature as $\xi_{ion} = Q^*_{ion}/L_{1500}$, in units of erg^{-1} Hz (see Mas-Hesse & Kunth 1991) for an analysis of the evolution of the equivalent B parameter as a function of the star formation scenario. Since we are dealing with Lyα EWs in Å, the following conversion applies: $\xi_{ion}(erg^{-1}Hz) = 1.35 \times 10^{23}$ EW(Lyα) (Å). The average intrinsic value derived by Sobral & Matthee (2019), EW(Lyα) ~200 Å, corresponds to log (ξ_{ion}) = 25.43 erg^{-1} Hz. We show in Fig. 2 (bottom) the evolution of ξ_{ion} for an instantaneous burst and an extended episode of star formation.

3.2 The number of LyC photons from the medium-luminosity galaxies in the BDF

To derive the number of ionizing continuum photons generated by the LBGs in the BDF, we have computed first their luminosities in the rest UV band. We expect that all the sources are within a redshift range of $6.95 < z < 7.15$. This assumes that the galaxies in the observed BDF are part of the same structure (Castellano et al. 2018). Indeed, as there is no spectroscopic confirmation, precise redshifts of the sources are not known. For convenience, we will assume the central wavelength of the Y105 filter, used for their discovery, as

Downloaded from https://academic.oup.com/mnras/article/503/3/4242/6155040 by guest on 12 February 2026

Table 2. Ly α emitters in the BDF. Name, group, Ly α rest-frame EW, Ly α flux, $f_{\mathrm{esc,Ly}\,\alpha}$, observed $L_{\mathrm{Ly}\,\alpha}$ luminosity, intrinsic $L_{\mathrm{Ly}\,\alpha}$ luminosity, and effective number of ionizing continuum photons per second, $Q^{e}_{\mathrm{ion,LAE}}$, respectively, of the three bright Ly α emitting galaxies in Castellano et al. (2018).

Name	Group	$\mathrm{EW_o}$ (Å)	$\mathrm{Flux_{Ly\,\alpha}}$ (10^{-17} erg s^{-1})	$f_{\mathrm{esc,Ly}\,\alpha}$	$L_{\mathrm{Ly}\,\alpha}$ (10^{42} erg s^{-1})	$\mathrm{L_{Ly\,\alpha,intr}}$ (10^{43} erg s^{-1})	$Q^{e}_{\mathrm{ion,LAE}}$ (10^{54} s^{-1})
BDF521	1	64 ± 6	1.62 ± 0.16	0.32 ± 0.03	9.14 ± 0.91	2.98 ± 0.41	2.53 ± 0.35
BDF2195	1	50 ± 12	1.85 ± 0.46	0.24 ± 0.06	10.56 ± 2.63	4.40 ± 1.52	3.73 ± 1.29
BDF3299	2	50 ± 6	1.21 ± 0.14	0.24 ± 0.24	7.08 ± 0.83	2.95 ± 0.49	2.50 ± 0.42

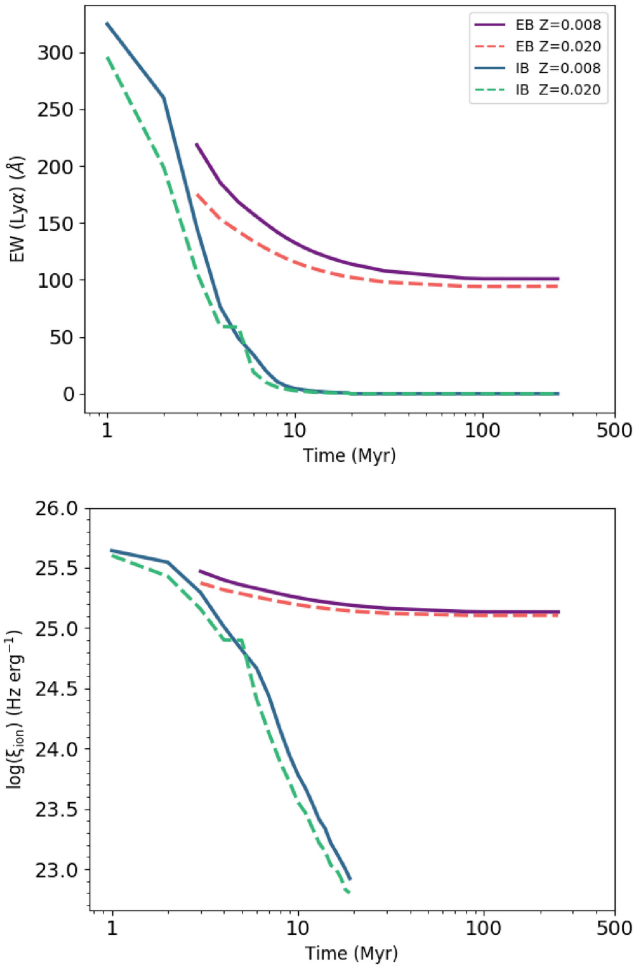


Figure 2. Ly α EW (top) and ξ_{ion} (bottom) evolution for instantaneous (IB) and extended (EB) episodes of star formation, for solar and subsolar metallicities, as predicted by Otí-Floranes & Mas-Hesse (2010). These models were based on the evolutionary code discussed by Cerviño, Mas-Hesse & Kunth (2002) for instantaneous bursts, and on STARBURST99 (Leitherer et al. 1999) for extended episodes of star formation. In both cases, they assumed a Salpeter initial mass function with an upper mass limit of 120 $\mathrm{M_\odot}$.

corresponding to the continuum at rest 1310 Å, at the redshift of 7.008. We have derived the f_{1310} directly from the AB magnitudes given by Castellano et al. (2018) correcting the fluxes to the rest-frame wavelength, and computing L_{1310} assuming that $z = 7.008$ is valid for all galaxies. We have assumed that $L_{1500} = 0.88 \times L_{1310}$ (corresponding to the mean UV continuum slope expected from a population of young, massive stars, with no extinction), and have used the predictions from the evolutionary models of Otí-Floranes & Mas-Hesse (2010), as available in their webtool,[1] to estimate the number of LyC photons being produced by the stars, for each value of the UV continuum luminosity. This webtool allows us to estimate the intrinsic number of continuum ionizing photons emitted by the starburst as a function of various parameters, including L_{1500}, and for different star formation scenarios.

Since the LBGs have no Ly α emission detected, we do not have any hint that these galaxies could be experiencing a very young star formation episode. If we assume that these galaxies are in any case experiencing a recent, or still active, episode of massive star formation, their intrinsic EW(Ly α) (or ξ_{ion}) values should be in between the predictions for the two scenarios considered in Fig. 2: a very young instantaneous burst or an extended episode having already reached an equilibrium between the birth and death of the most massive stars, i.e. active during more than around the last 50 Myr. After this time, the EW(Ly α) evolves very slowly and can be considered constant for up to around 1 Gyr, longer than the age of the universe at $z \sim 7$ (see also the predictions by Charlot & Fall 1993). Otí-Floranes & Mas-Hesse (2010) predict that the Ly α EW would converge to EW(Ly α) $\sim$ 95–101 Å [or $\log(\xi_{\mathrm{ion}}) \sim 25.10$–$25.13$ erg^{-1} Hz] for metallicities in the range of $Z = 0.020$–0.008. The weak dependence on metallicity is related to the fact that as the massive stellar population stabilizes with time, both the ionizing and the UV continuum flux of low-metallicity stars increase when compared to solar metallicity, so that the effect on the EW(Ly α) is partially compensated.

We have therefore assumed as our initial scenario the more conservative option of an extended star forming process having reached the equilibrium phase. In Table 3, we list the derived luminosities at rest 1500 Å, L_{1500}, and the corresponding number of ionizing continuum photons (Q^{*}_{ion}) value, as estimated with the webtool for extended episodes at 250 Myr, assuming an intrinsic EW(Ly α) $\sim$ 100 Å. Note that we have corrected Q^{*}_{ion} from the standard 30 per cent destruction factor assumed by the Otí-Floranes & Mas-Hesse (2010) models, not applicable to high-redshift, low-dust galaxies. We insist that since we are dealing with EWs, which are tracing the ionizing power per UV luminosity unit, our estimates are essentially independent of the precise history of star formation, but are only scaled to the UV continuum luminosity. The same Q^{*}_{ion} values would be derived for star formation episodes with stable rates during the last 50–500 Myr. On the other hand, the predictions for an instantaneous burst should provide the expected upper limit if the star formation rate has suffered a very recent, significant increase in the last 1–5 Myr.

The assumed intrinsic Ly α value [EW(Ly α) $\sim$ 100 Å, or $\log \xi_{\mathrm{ion}} \sim 25.13$ erg^{-1} Hz] is very similar to the canonical values of Kennicutt (1998), $\log \xi_{\mathrm{ion}} = 25.11$ erg^{-1} Hz (see Bouwens et al. 2016). We want to stress that most of these values are well

[1] http://sfr.cab.inta-csic.es/index.php

Downloaded from https://academic.oup.com/mnras/article/503/3/4242/6155040 by guest on 12 February 2026

Table 3. LBGs in the BDF with no Ly α emission detected. (1) Name, (2) group, (3) observed magnitude $M_{\rm AB}$, flux at λ1310 rest frame, (4) luminosity at λ1500, and (5) the number of intrinsic LyC photons emitted per second assuming an extended episode of star formation (Otí-Floranes & Mas-Hesse 2010).

Name	Group	$M_{\rm AB}$	$f_{\lambda 1310}$ (10^{-20} erg s^{-1} cm^{-2} Å^{-1})	L_{1500} (10^{40} erg s^{-1} Å^{-1})	$Q^*_{\rm ion,LBG}$ (10^{54} s^{-1})
BDF2009	1	26.89 ± 0.08	13.75 ± 12.78	6.89 ± 5.61	0.65 ± 0.50
BDF994	1	27.11 ± 0.19	11.23 ± 9.43	5.69 ± 4.19	0.53 ± 0.39
BDF2660	1	27.27 ± 0.10	9.69 ± 8.84	4.91 ± 3.93	0.46 ± 0.34
BDF1310	1	27.32 ± 0.16	9.26 ± 7.99	4.69 ± 3.55	0.44 ± 0.31
BDF187	1	27.33 ± 0.10	9.17 ± 8.37	4.65 ± 3.72	0.43 ± 0.33
BDF1899	1	27.35 ± 0.15	9.00 ± 7.84	4.56 ± 3.49	0.42 ± 0.31
				Total Group 1	**2.93 ± 0.15**
BDF2883	2	25.97 ± 0.08	32.10 ± 29.82	16.08 ± 14.94	1.51 ± 1.32
BDF401	2	26.43 ± 0.08	21.01 ± 19.52	10.53 ± 9.78	0.99 ± 0.87
BDF1147	2	27.26 ± 0.11	9.78 ± 8.84	4.72 ± 4.23	0.46 ± 0.39
BDF2980	2	27.30 ± 0.12	9.43 ± 8.44	4.72 ± 4.23	0.44 ± 0.38
BDF647	2	27.31 ± 0.15	9.34 ± 8.14	4.68 ± 4.08	0.44 ± 0.36
BDF2391	2	27.33 ± 0.17	9.17 ± 7.84	4.59 ± 3.93	0.43 ± 0.35
BDF1807	2	27.36 ± 0.09	8.92 ± 8.21	4.47 ± 4.11	0.42 ± 0.36
BDF2192	2	27.40 ± 0.10	8.60 ± 7.84	4.31 ± 3.93	0.41 ± 0.35
				Total Group 2	**5.11 ± 0.64**

Table 4. Non-detected low-luminosity sources. Columns: (1) average magnitude AB, (2) flux at 1310 Å, (3) continuum luminosity at 1500 Å, (4) the number of ionizing continuum photons, once corrected for the number of sources and overdensity for Group 1, and (5) for Group 2.

$m_{\rm AB}$	$f_{\lambda 1310}$ $\times 10^{-20}$ (erg s^{-1} cm^{-2} Å^{-1})	L_{1500} $\times 10^{40}$ (erg s^{-1})	$Q^*_{\rm ion,G1}$ $\times 10^{54}$ (s^{-1})	$Q^*_{\rm ion,G2}$ $\times 10^{54}$ (s^{-1})
27.70	6.74	3.38	3.64 ± 0.38	3.53 ± 0.27
28.20	4.25	2.13	3.52 ± 0.30	3.41 ± 0.21
28.70	2.68	1.34	2.20 ± 0.33	2.14 ± 0.23
29.20	1.69	0.85	4.72 ± 0.38	4.57 ± 0.27
29.70	1.07	0.54	2.42 ± 0.22	2.35 ± 0.15
Total			16.49 ± 0.39	15.99 ± 0.27

constrained by the predictions of our evolutionary models as shown in Fig. 2.

3.3 The output from the low-luminosity sources

Likewise, we have derived the number of LyC photons for the expected, non-detected, lower luminosity sources, which play an essential role in producing the ionizing photons required to reionize the Universe (Bouwens et al. 2015; Higuchi et al. 2019; Tilvi et al. 2020). First, we have computed the luminosity at 1500 Å corresponding to the middle AB magnitude for each of the magnitude ranges listed in Table 1, following the same procedure as in the previous section. Thus, using a similar methodology as in the case of the medium-luminosity galaxies, we have derived the expected number of ionizing continuum photons corresponding to each AB magnitude bin, considering the total number of expected galaxies in each magnitude range as listed in Table 1. We list in Table 4 the derived number of intrinsic ionizing continuum photons expected from the low-luminosity galaxies. When compared with the contributions by the LAEs and LBGs in the sample, it becomes evident that faint galaxies indeed dominate the release of ionizing photons to the IGM, as already proposed by Bouwens et al. (2016), Castellano et al. (2018), and Robertson et al. (2013). We would like finally to remind that these estimates should be considered as lower limits, since we have assumed extended star formation episodes in their equilibrium phase, as for the LBGs in the previous section, with canonical values for the ionizing photon production efficiency. We will discuss in Section 4.1 the effect of other possible scenarios.

Table 5. The number of intrinsic ionizing continuum photons produced by the medium- and low-luminosity LBGs in each of the groups. The values listed for the LAEs are just lower limits as they should be corrected by the corresponding LyC escape fraction as discussed in the text.

	$Q^*_{\rm ion,G1}$ $\times 10^{54}$ s^{-1}	$Q^*_{\rm ion,G2}$ $\times 10^{54}$ s^{-1}
LAEs	$\gtrsim$6.26 ± 0.94	$\gtrsim$2.50 ± 0.42
Mid luminosity	2.93 ± 0.15	5.11 ± 0.64
Low luminosity	16.49 ± 0.39	15.99 ± 0.27
Total	$\lesssim$25.68 ± 0.59	$\lesssim$23.60 ± 0.47

4 DISCUSSION

A non-zero LyC escape fraction implies that the escaping photons will be able to ionize regions farther out from the galaxy or galaxies that contain the massive stars producing the ionizing photons. Adding to the number of ionizing continuum photons produced by the LAEs the contribution by the medium- and low-luminosity star-forming galaxies for both Group 1 and Group 2 in the BDF, we arrive to a total number of ionizing continuum photons of $\gtrsim 25.68 \pm 0.59 \times 10^{54}$ s^{-1} for Group 1 and $\gtrsim 23.60 \pm 0.47 \times 10^{54}$ s^{-1} for Group 2, as listed in Table 5. We remark that for the LAEs we do not yet know the intrinsic number of ionizing continuum photons emitted per second, since it depends on the actual LyC escape fraction.

The next step is to derive the minimum number of ionizing continuum photons necessary to fully ionize the volumes of both Group 1 and Group 2. We get these values by multiplying the ionizing emissivities derived from the AMIGA model (Salvador-Solé et al. 2017) by the volumes of Group 1 and Group 2. AMIGA is a very complete and detailed self-consistent model of galaxy formation, particularly well suited to monitor the intertwined evolution of both luminous sources and the IGM. It computes the instantaneous emis-

Downloaded from https://academic.oup.com/mnras/article/503/3/4242/6155040 by guest on 12 February 2026

Table 6. LyC escape fractions derived for Group 1 and Group 2 in the single and double reionization scenarios. These escape fractions are enough to fully ionize both regions.

	$\dot{N}^{S}_{\rm min,corr}$ $\times 10^{54}$ s^{-1}	$\dot{N}^{D}_{\rm min,corr}$ $\times 10^{54}$ s^{-1}	$f_{\rm esc,S}$	$f_{\rm esc,D}$
Group 1	2.20 ± 0.09	3.01 ± 0.09	0.08	0.10
Group 2	2.12 ± 0.08	2.91 ± 0.08	0.12	0.14

sion at all the relevant wavelengths of normal galaxies, including their intrinsic ionizing power, using the evolutionary synthesis models by Bruzual & Charlot (2003), assuming a Salpeter initial mass function. The parameters in the AMIGA model have been tuned to reproduce as well as possible the properties of high-redshift star-forming galaxies, including the contribution of very low metallicity Pop III stars in the early epochs. Therefore, the average ionizing emissivities derived from AMIGA should provide a fair estimate of the number of ionizing continuum photons necessary to ionize the IGM at $z \sim 7$. AMIGA distinguishes between the most usual case of single reionization, plus the less usual case of double reionization. These emissivities, as derived from AMIGA, are $0.26 \pm 0.01 \times 10^{51}$ s^{-1} cMpc^{-3} for the single reionization scenario and $0.36 \pm 0.01 \times 10^{51}$s^{-1} cMpc^{-3} for the double reionization case.

Though the AMIGA simulations include already the presence of clumpiness, the predicted emissivities correspond to average values over the IGM at $z \sim 7$. Since the two regions we are considering in the BDF seem to be overdense by a factor of 3–4 (Castellano et al. 2016), we consider that the density of ionizing photons should also be larger by a factor of ∼3.5 to fully reionize the local IGM. We have therefore multiplied the emissivities derived from AMIGA by 3.5 to properly take this effect into account. Moreover, since the average ionized fraction of the IGM predicted by AMIGA at $z \sim 7$ is only ∼0.7 for both the single and double reionization scenarios, we have divided the emissivities by this value to account for a fully reionized IGM.

The emissivities after these corrections are $1.28 \pm 0.05 \times 10^{51}$ s^{-1} cMpc^{-3} for single reionization and $1.75 \pm 0.05 \times 10^{51}$ s^{-1} cMpc^{-3} for double reionization. Finally, multiplying these emissivities by the volumes of each of the groups we derive the minimum number of continuum ionizing photons per second required to completely ionize those volumes. The resulting values are $2.20 \pm 0.09 \times 10^{54}$ s^{-1} for Group 1 and $2.12 \pm 0.09 \times 10^{54}$ s^{-1} for Group 2 in the case of single reionization. For the case of double reionization, the values are $3.01 \pm 0.09 \times 10^{54}$ s^{-1} for Group 1 and $2.91 \pm 0.08 \times 10^{54}$ s^{-1} for Group 2, as listed in Table 6.

The total number of photons available for reionizing the circumgalactic medium will depend on the LyC escape fraction, $f_{\rm esc,LyC}$. We can constrain the average value required to fully reionize the volumes around Group 1 and Group 2 by comparing the yield of ionizing photons we have derived with the predictions by AMIGA, i.e. by solving equation (1), as follows:

$$\left\{ Q^{*}_{\rm ion} + \frac{Q^{e}_{\rm ion,LAE}}{1 - f_{\rm esc,LyC}} \right\} \times f_{\rm esc,LyC} = \dot{\rm N}_{\rm min,corr}. \quad (1)$$

The first term of equation (1) corresponds to the intrinsic number of ionizing continuum photons produced by the massive stars in the medium- and low-luminosity galaxies. The second term concerns the LAEs. In the case of the LAEs, to derive the intrinsic number of LyC photons we have to divide the *effective* number by $\frac{1}{1-f_{\rm esc,LyC}}$. Then, we multiply these two terms by the LyC escape fraction to get the number of continuum ionizing photons available to ionize the IGM. Finally, the term at the other side of equation (1) is the emissivity derived from the AMIGA model, multiplied by the volumes of each group, and corrected by both the overdensity and ionization fraction at $z \sim 7$.

The results, as shown in Table 6, indicate that the volumes of Group 1 and Group 2 in the BDF would be completely ionized if the escape fractions of LyC photons are as low as 0.08 for Group 1 and 0.12 for Group 2, in the case of single reionization. For the case of double reionization, the two groups would be fully ionized if the $f_{\rm esc,LyC}$ values are 0.10 and 0.14, respectively. These are rather low values of the average LyC escape fractions. Our method allows us to constrain the average $f_{\rm esc,LyC}$ value, but we want to stress that values for specific galaxies can vary significantly. Finkelstein et al. (2019) proposed that $f_{\rm esc,LyC}$ should be inversely correlated with the halo mass of the individual galaxies, thus $f_{\rm esc,LyC}$ becoming significantly higher for galaxies with $M_{\rm h} < 10^{7.5}$ M$_{\odot}$ (see their figure 2). Since the main contributors to the ionizing power in the BDF are the low-luminosity galaxies, we interpret our results in the sense that the derived $f_{\rm esc,LyC}$ values should represent the typical values for the low-mass galaxies.

Such low values of $f_{\rm esc,LyC}$ are consistent with the fact that there are only three LAEs in the BDF. According to Chisholm et al. (2018), we should expect similar low values of $f_{\rm esc,LyC}$ and $f_{\rm esc,Ly\,\alpha}$ in galaxies with low extinction by dust, as should be the case at $z \sim 7$ (Hayes et al. 2011). With an average $f_{\rm esc,LyC} \sim 0.1$, and following Chisholm et al. (2018) and the calibration by Sobral & Matthee (2019), we would expect EW(Ly α) ∼ 20 Å, which is too low to be detected on the BDF observations. Nevertheless, the large dispersion expected in $f_{\rm esc,Ly\,\alpha}$ (Dijkstra et al. 2016) would support the presence of some galaxies with larger values of the Ly α escape fraction, which would come out as the three LAEs identified in the BDF.

4.1 A large ionized bubble in the BDF

We want to stress that our analysis has been rather conservative when deriving the number of intrinsic ionizing photons emitted by the galaxies in the BDF. The calibration of $f_{\rm esc,Ly\,\alpha}$ versus the rest-frame EW(Ly α) by Sobral & Matthee (2019) for the LAEs implies an average intrinsic value of the Ly α equivalent around ∼200 Å, corresponding to log $\xi_{\rm ion} \sim 25.43$ erg^{-1} Hz, while Harikane et al. (2018) find an average log $\xi_{\rm ion} \sim 25.53$ erg^{-1} Hz (and $f_{\rm esc,LyC} \sim 0.10$) for a large sample of LAEs at $z \sim 4.9$–7.0. On the other hand, as discussed above, the assumed intrinsic Ly α value EW(Ly α) ∼ 100 Å for the LBGs corresponds to log $\xi_{\rm ion} \sim 25.13$ erg^{-1} Hz. Bouwens et al. (2016) derived average values log $\xi_{\rm ion} \sim 25.3$ erg^{-1} Hz for a sample of galaxies with *Spitzer* H α IRAC observations at $z \sim 4$–5, with an intrinsic scatter of ∼0.3 dex for individual galaxies. The UV continuum bluest galaxies in the sample reached log $\xi_{\rm ion} \sim 25.5$–25.8 erg^{-1} Hz, indicating that $f_{\rm esc,LyC}$ cannot be in excess of 0.13. Stark et al. (2015) derived log $\xi_{\rm ion} = 25.68$ erg^{-1} Hz from the C IV λ1548 observations of A1703-zd6, a galaxy at $z = 7.045$ with Ly α EW$_{\rm o} \sim$ 65 Å (Schenker et al. 2012), and Stark et al. (2017) derived log $\xi_{\rm ion} \sim$ 25.58 erg^{-1} Hz for three luminous ($M_{\rm UV} = -22$) galaxies at $z = 7.15$, 7.48, and 7.73. Moreover, Bouwens et al. (2015) estimate log $\xi_{\rm ion} =$ 25.46 erg^{-1} Hz for faint galaxies at $z \sim$ 7–8, with an associated $f_{\rm esc,LyC} \sim 0.11$, to properly match the reionization timeline of the Universe. Finally, Wilkins et al. (2016) constrained log $\xi_{\rm ion}$ during the reionization epoch to the range 25.1–25.5 erg^{-1} Hz by combining the BlueTides cosmological hydrodynamical simulation with a range of stellar population synthesis models.

Large values of the intrinsic EW(Ly α) or $\xi_{\rm ion}$ can be associated with very young star formation episodes (or with a sudden increase

Downloaded from https://academic.oup.com/mnras/article/503/3/4242/6155040 by guest on 12 February 2026

of the star formation rate in the last ∼10 Myr) or the presence of very low metallicity stars. Schaerer (2003) showed that for metallicities down to $Z \sim 10^{-7}$ the intrinsic values of EW(Ly α) can reach up to EW(Ly α) $\sim$ 250–300 Å for stable star formation rates in the equilibrium phase, and even higher values for lower metallicities and/or larger values of the initial mass function upper mass limit. Combining all these observational results and model predictions, we consider that the intrinsic EW(Ly α) values of the LAEs, LBGs, and low-luminosity galaxies we have used in our calculations could realistically be increased by a factor of 4 at most. Keeping $f_{\rm esc,LyC} \sim 0.1$, as constrained by the results discussed above, this would lead to a total number of ionizing continuum photons released to the IGM of 1.05×10^{55} s^{-1} for Group 1 and 0.96×10^{55} s^{-1} for Group 2, i.e. a total $Q^{*}_{\rm ion} \sim 2 \times 10^{55}$ s^{-1}.

Comparing these numbers with the AMIGA emissivities listed in Table 6, we conclude that an IGM volume 4.6 times (single reionization) or 3.4 times (for double reionization) larger than the volumes of Group 1 and Group 2 together would become reionized assuming larger, but still realistic, values of the ionizing power for the star-forming galaxies in the two BDF overdensities. Since the volume comprising both overdensities (extended over 30 arcmin^2) would be roughly a factor of ∼4 larger than the added volume of both groups, there would be enough ionizing photons released to the IGM for the two ionized bubbles around them to merge in a single, very large reionized bubble.

We conclude that realistic, rather small values of the LyC escape fractions would allow us to completely reionize the overdense regions of the BDF within a single, large ionized bubble, such as those that through percolation completed the reionization of the universe by $z \sim 6$. On the other hand, the still required presence of neutral gas around the star-forming regions in these galaxies, evidenced by the low values of the escape fractions, would explain the scarcity of detected faint LAEs, since the observed EW(Ly α) values would remain, on average, rather low.

5 CONCLUSIONS

We have looked for the reionization status of the IGM around two overdense groups of star-forming galaxies in the BDF. To this end, we have considered all the sources in the BDF, including galaxies that are expected but have not yet been detected. These are low-luminosity sources, for which we have estimated their numbers in the BDF assuming the average surface density at $z \sim 7$ from Bouwens et al. (2015) and an overdensity of 3.5x, as estimated by Castellano et al. (2016). Then, we have derived the number of intrinsic ionizing photons from the bright LAEs and the medium-luminosity LBGs identified by Castellano et al. (2018), to which we have added the contribution of the expected low-luminosity sources. Even adopting conservative estimates for the ionizing continuum photons produced by the massive stars in all these sources, known and expected, we conclude that there would be enough photons to ionize two large bubbles, one per group in the BDF, with average LyC escape fraction as low as $f_{\rm esc,LyC} \sim 0.08$ for Group 1 and 0.12 for Group 2. With less conservative, but more realistic, estimates of the ionizing power, the two bubbles would be merging into a large ionized bubble comprising most of the galaxies in the BDF. These low values of the LyC escape fraction indicate that there are still substantial amounts of neutral hydrogen surrounding the star-forming regions in these galaxies. The inferred low values of the $f_{\rm esc,Ly\,\alpha}$ would explain the scarcity of faint LAEs found within the none the less completely reionized bubbles. We confirm previous hints indicating that the low-luminosity sources are indeed the ones that dominate the reionization of the BDF. Finally, we note that a scenario with a double reionization would require only slightly larger LyC escape fractions than the more commonly assumed single reionization.

ACKNOWLEDGEMENTS

We are very grateful to Sonia Torrejón de Pablos for having computed the EW(Ly α) predictions plotted in Fig. 2. We are also very grateful to Dr Alberto Manrique (University of Barcelona) for sharing his values of the AMIGA emissivities. JMRE acknowledges the Spanish State Research Agency under grant number AYA2017-84061-P and is indebted to the Severo Ochoa Programme at the IAC. JMMH was funded by Spanish State Research Agency grants PID2019-107061GB-C61 and MDM-2017-0737 (Unidad de Excelencia María de Maeztu CAB).

DATA AVAILABILITY

All the LAE fluxes and rest-frame EW(Ly α) values, as well as the medium-luminosity LBG magnitudes, are available in Castellano et al. (2018). The low-luminosity source data are new in this paper.

REFERENCES

Abdullah M. H., Wilson G., Klypin A., 2018, ApJ, 861, 22
Bouwens R. J., Illingworth G. D., Blakeslee J. P., Franx M., 2006, ApJ, 653, 53
Bouwens R. J. et al., 2010, ApJ, 725, 1587
Bouwens R. J. et al., 2015, ApJ, 803, 34
Bouwens R. J., Smit R., Labbé I., Franx M., Caruana J., Oesch P., Stefanon M., Rasappu N., 2016, ApJ, 831, 176
Bouwens R. J., Oesch P. A., Illingworth G. D., Ellis R. S., Stefanon M., 2017, ApJ, 843, 129
Bruzual G., Charlot S., 2003, MNRAS, 344, 1000
Calvi R. et al., 2019, MNRAS, 489, 3294
Castellano M. et al., 2016, ApJ, 818, L3
Castellano M. et al., 2018, ApJ, 863, L3
Cerviño M., Mas-Hesse J. M., Kunth D., 2002, A&A, 392, 19
Chanchaiworawit K. et al., 2017, MNRAS, 469, 2646
Chanchaiworawit K. et al., 2019, ApJ, 877, 51
Charlot S., Fall S. M., 1993, ApJ, 415, 580
Chiang Y.-K., Overzier R. A., Gebhardt K., Henriques B., 2017, ApJ, 844, L23
Chisholm J. et al., 2018, A&A, 616, A30
Dijkstra M., Gronke M., Venkatesan A., 2016, ApJ, 828, 71
Dopita M. A., Sutherland R. S., 2003, Astrophysics of the Diffuse Universe, Astronomy and Astrophysics Library
Finkelstein S. L. et al., 2019, ApJ, 879, 36
Harikane Y. et al., 2018, ApJ, 859, 84
Harikane Y. et al., 2019, ApJ, 883, 142
Hayes M., 2019, in Verhamme A., North P., Cantalupo S., Atek H., eds, Lyman-Alpha as an Astrophysical and Cosmological Tool. Springer, Berlin, p. 319
Hayes M., Schaerer D., Östlin G., Mas-Hesse J. M., Atek H., Kunth D., 2011, ApJ, 730, 8
Higuchi R. et al., 2019, ApJ, 879, 28
Jiang L. et al., 2018, Nat. Astron., 2, 962
Kennicutt Robert C. J., 1998, ApJ, 498, 541
Leitherer C. et al., 1999, ApJS, 123, 3
Mas-Hesse J. M., Kunth D., 1991, A&AS, 88, 399
Meyer R. A., Laporte N., Ellis R. S., Verhamme A., Garel T., 2020, MNRAS, 500, 558
Oke J. B., Gunn J. E., 1983, ApJ, 266, 713
Osterbrock D. E., 1989, Ann. New York Acad. Sci., 571, 99
Oteo I. et al., 2018, ApJ, 856, 72

Downloaded from https://academic.oup.com/mnras/article/503/3/4242/6155040 by guest on 12 February 2026

Otí-Floranes H., Mas-Hesse J. M., 2010, A&A, 511, A61
Ouchi M. et al., 2008, ApJS, 176, 301
Ouchi M. et al., 2010, ApJ, 723, 869
Robertson B. E. et al., 2013, ApJ, 768, 71
Robertson B. E., Ellis R. S., Furlanetto S. R., Dunlop J. S., 2015, ApJ, 802, L19
Rodríguez Espinosa J. M. et al., 2020, MNRAS, 495, L17
Salvador-Solé E., Manrique A., Guzman R., Rodríguez Espinosa J. M., Gallego J., Herrero A., Mas-Hesse J. M., Marín Franch A., 2017, ApJ, 834, 49
Schaerer D., 2003, A&A, 397, 527
Schenker M. A., Stark D. P., Ellis R. S., Robertson B. E., Dunlop J. S., McLure R. J., Kneib J.-P., Richard J., 2012, ApJ, 744, 179
Sobral D., Matthee J., 2019, A&A, 623, A157
Stark D. P., Ellis R. S., Chiu K., Ouchi M., Bunker A., 2010, MNRAS, 408, 1628
Stark D. P. et al., 2015, MNRAS, 454, 1393
Stark D. P. et al., 2017, MNRAS, 464, 469
Steidel C. C., Adelberger K. L., Shapley A. E., Erb D. K., Reddy N. A., Pettini M., 2005, ApJ, 626, 44
Tilvi V. et al., 2020, ApJ, 891, L10
Toshikawa J. et al., 2012, ApJ, 750, 137
Vanzella E. et al., 2011, ApJ, 730, L35
Verhamme A., Orlitová I., Schaerer D., Izotov Y., Worseck G., Thuan T. X., Guseva N., 2017, A&A, 597, A13
Wilkins S. M., Feng Y., Di-Matteo T., Croft R., Stanway E. R., Bouwens R. J., Thomas P., 2016, MNRAS, 458, L6
Wright E. L., 2006, PASP, 118, 1711
Yue B. et al., 2018, ApJ, 868, 115

This paper has been typeset from a TEX/LATEX file prepared by the author.

Downloaded from https://academic.oup.com/mnras/article/503/3/4242/6155040 by guest on 12 February 2026